296 Chem. Mater. 1992, 4, 296-307

Synthesis and Structure of Borazinyl-Substituted Small-Molecule and High Polymeric Phosphazenes: Ceramic Precursors

Harry R. Allcock,* Mark F. Welker, and Masood Parvez

Department of Chemistry, The Pennsylvania State University, University Park, Pennsylvania 16802

Received July 9, 1991. Revised Manuscript Received January 16, 1991

Mixed-substituent small-molecule cyclic and high molecular weight polymeric (borazinylamino)phosphazenes have been prepared by reactions between aminophosphazenes and chloroborazines as well as between chlorophosphazenes and aminoborazines. A single-crystal X-ray diffraction study of a small-molecule model compound, *gem*-bis(borazinylamino)cyclotriphosphazene, $N_3P_3(NMe_2)_4(NHB_3N_3Me_5)_2$ (**10**), is reported: triclinic, space group $P1$, $a = 9.424$ (2) Å, $b = 13.841$ (1) Å, $c = 14.570$ (4) Å, $\alpha = 79.40$ (1)°, $\beta = 83.44$ (2)°, $\gamma = 73.99$ (1)°, $V = 1791.5$ Å^3, $Z = 2$, $D_c = 1.187$ g cm^{-3}, Mo Kα radiation, $\lambda = 0.71073$ Å, $\mu = 0.196$ mm^{-1}, $R = 0.066$. The exocyclic P–N and B–N bond lengths of the borazinylamino substituents indicate significant delocalization of the nitrogen atom lone pair, with preference into the borazinyl ring rather than the phosphazene ring. Pyrolysis studies of the mixed-substituent (borazinylamino)phosphazene polymers indicate that these polymers are potential precursors to new ceramic materials, with up to 57% ceramic yield when heated to 1000 °C under nitrogen. Continued pyrolysis at 1300 °C for 10 h leads to the production of crystalline hexagonal boron nitride.

Introduction

In recent years, polymers that contain main-group inorganic elements have served as precursors for pyrolysis to non-oxide ceramic materials. This method underlies the synthesis of several important ceramics such as SiC, Si_3N_4, BN, and B_4C.[1-14] Earlier work has shown the importance of identifying and developing suitable polymeric precursors, as well as the determination of optimum pyrolysis conditions. These developments have stimulated increased interest in the synthesis of new preceramic polymers and oligomers that possess inorganic rings or chains. Entirely new precursors are needed for the development of several desirable boride, phosphide, and nitride ceramics for which no feasible syntheses currently exist.[3]

The ultimate goal of advanced ceramic synthesis is the conversion of small molecules to highly cross-linked ultrastructures. This involves the conversion of volatile, low melting, reactive small molecules to nonvolatile, unreactive, two- or three-dimensionally connected materials, by pathways that allow shaping and fabrication at some intermediate step in the process. For practical reasons it is also desirable to minimize the weight loss that occurs during the synthesis process.

Scheme I

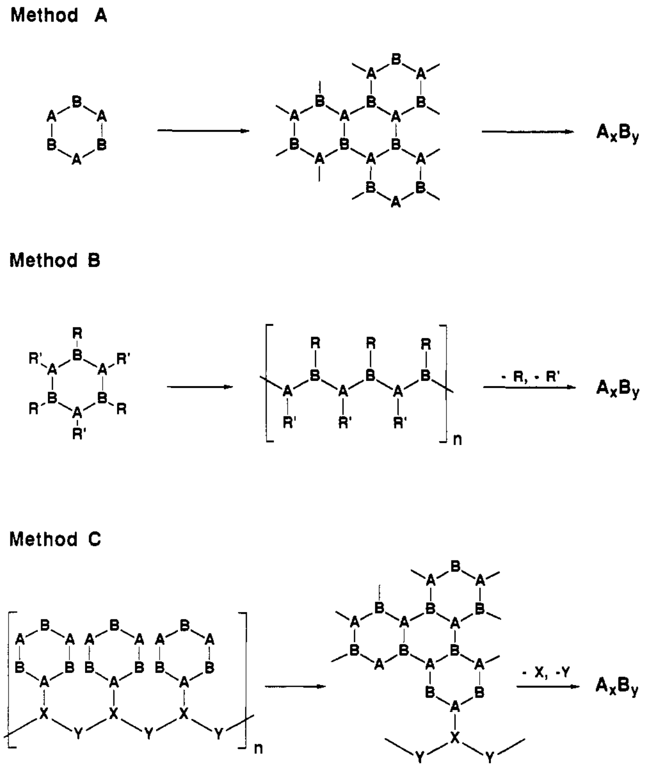

In most cases the methodology involves the conversion of inorganic ring systems to ceramics via the intermediate formation of polymers. The polymer stage provides the necessary materials strength to permit fabrication. There are three variants of the general processes for the conversion of inorganic small molecules to macromolecular species and eventually to ceramics, and these are illustrated in Scheme I. The main differences between these routes are outlined below.

The first method involves the linkage of inorganic ring systems to form preceramic oligomers or "clusters" (method A). These clusters are not polymers in the true sense of the word since they usually contain relatively few (often 10–50) ring systems linked together, rather than the thousands of repeating units that are usually associated with polymers. Moreover, they often have dendritic rather

---

(1) Yajima, S.; Hasegawa, Y.; Okamura, K.; Matsuzowa, T. *Nature* 1978, *273*, 525.

(2) Rice, R. W. *Ceram. Bull.* 1983, *62*, 889.

(3) Wynne, K. J.; Rice, R. W. *Annu. Rev. Mater. Sci.* 1984, *14*, 297.

(4) Seyferth, D.; Wiseman, G. H.; Schwark, J. M.; Yu, Y. F.; Poutasse, C. A. In *Inorganic and Organometallic Polymers*; Zeldin, M., Wynne, K. J., Allcock, H. R., Eds.; ACS Symp. Ser. 360; American Chemical Society: Washington, DC, 1988; p 143.

(5) Arai, M.; Sakurada, S.; Isoda, T.; Tomizawa, T. *Polym. Prepr.* (*Am. Chem. Soc., Polym. Div.*) 1987, *27*, 47.

(6) Laine, R. M.; Blum, Y. D.; Tse, T.; Glaser, R. In ref 4, p 124.

(7) Yajima, S.; Hayashi, J.; Omori, M. *Chem. Lett.* 1975, 1209.

(8) West, R.; Maxha, J. In ref 4, p 6.

(9) Sneddon, L. G.; Mirabelli, M. G. L. *Inorg. Chem.* 1988, *27*, 3271.

(10) Sneddon, L. G.; Lynch, A. T. *J. Am. Chem. Soc.* 1989, *111*, 6201.

(11) Sneddon, L. G.; Lynch, A. T.; Remsen, E. E.; Beck, J. S.; Fazen, P. J. *Chem. Mater.* 1990, *2*, 96.

(12) Paine, R. T.; Narula, C. K.; Schaeffer, R.; Datye, A.; Hammetter, W. F. *J. Am. Chem. Soc.* 1987, *109*, 5557.

(13) Paciorek, K. J. L.; Schmidt, W. R.; Masuda, S. R.; Kratzer, R. H. *Chem. Mater.* 1991, *3*, 88.

(14) Paciorek, K. J. L.; Kratzer, R. H.; Kimble, P. F.; Nakahara, J. H.; Wynne, K. J. *Inorg. Chem.* 1988, *27*, 2432.

0897-4756/92/2804-0296$03.00/0

Scheme II

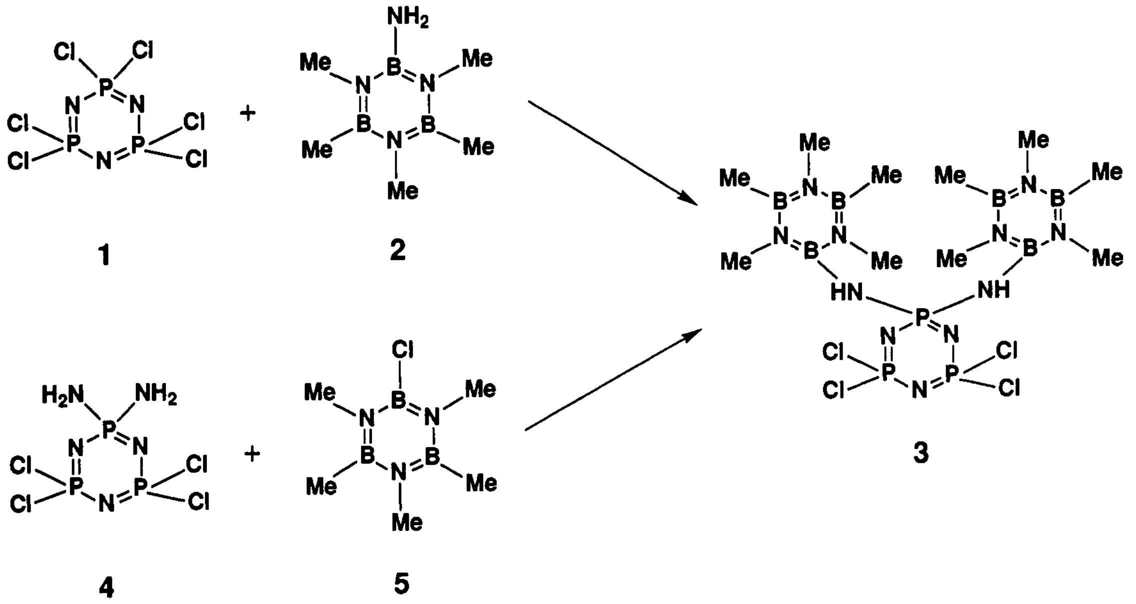

than linear or cyclolinear structures. Nevertheless, these clusters provide sufficient intermolecular entanglement to provide cohesion during the fabrication of the material. The preparation of Si_3N_4 from cyclosilazanes is an example of this principle.[4-6]

The second approach involves the ring-opening polymerization of inorganic cyclic molecules to give essentially linear, single-strand polymers (method B). These macromolecules can be solution- or melt-fabricated into fibers, films, or monolithic objects. Subsequent heating induces cross-linking at low-to-moderate temperatures. Continued pyrolysis eventually drives off the organic side group residues to leave an inorganic ceramic residue. The preparation of SiC from polysilanes is an example of this method.[7,8]

Finally, preceramic inorganic rings, or inorganic side groups that possess latent reactivity, may be linked to the backbone of a carrier polymer (method C). Heating of the polymer causes cross-linking of the inorganic side groups, while concurrent or subsequent thermolysis leads to the loss of the backbone through fragmentation and volatilization. Vinylboranes are converted to BN by this method.[9]

Borazines possess many of the desired characteristics for the development of methods A and C outlined in Scheme I, and there has been particular interest in the development of BN ceramics by the pyrolysis of oligomeric and polymeric precursors.[9-14]

Earlier work in our program has explored the possibility that polymers based on a phosphorus–nitrogen macromolecular chain might serve as precursors to phosphams, phosphorus nitride, or other ceramics that contain phosphorus, nitrogen, and other elements such as boron or transition metals.[15-19] The ability to design and modify the side-group structure of phosphazene polymers allows the synthesis of many new materials that provide a broad range of properties. Thus, given the wide range of polymers accessible, polyphosphazenes provide an attractive starting point for the design and synthesis of new ceramic-type materials. For example, phosphazenes that bear borazine units as side groups could serve as precursors to new phosphorus–nitrogen–boron ceramics or to boron nitride. Thus, in the present work, hybrid borazine–phosphazene oligomers and macromolecules have been synthesized. The precursor polymers to be discussed in this paper fall into category C of Scheme I.

Three major questions have been addressed in this study: First, what methods are accessible for the linkage of borazines as side groups to small-molecule cyclic phosphazenes? These species would be both synthetic and structural models for the corresponding high polymers. Second, what methods can be developed to prepare the corresponding high polymeric linear phosphazenes with borazinyl side groups? And finally, what processes take place when the polymers are heated to high temperatures? Optimization of the side-group ratios and the pyrolysis conditions are essential components of this work.

We report here the synthesis and characterization of the first (borazinylamino)phosphazene cyclic trimers, together with analogous high molecular weight linear (borazinylamino)phosphazene polymers.[20] Pyrolysis studies of the high molecular weight mixed substituent (borazinylamino)phosphazene polymers are described. Thermolysis of mixed substituent amino(dimethylamino)phosphazene polymers (model polymers that lack borazinyl side groups) are also discussed. The results of these studies indicate that the presence of borazinyl side groups enhances the overall thermal stability of phosphazene-based ultrastructures and that mixed-substituent (borazinylamino)phosphazene polymers are pyrolytic precursors to new P–N–B ceramic materials.

Results and Discussion

Small-Molecule Syntheses. Several synthetic routes to small-molecule model borazinylphosphazenes were investigated. These include attempts to link borazine units

---

(15) Allcock, H. R. *Phosphorus-Nitrogen Compounds*; Academic Press: New York, 1972.

(16) Allcock, H. R. *Chem. Eng. News* **1985**, *63*, 22.

(17) Allcock, H. R.; Desorcie, J. L.; Riding, G. H. *Polyhedron* **1987**, *6*, 119.

(18) Allcock, H. R. In *Ultrastructure Processing of Advanced Ceramics*; Mackenzie, J. D., Ulrich, D. R., Eds.; Wiley and Sons: New York, 1988; pp 705–713.

(19) Allcock, H. R.; McDonnell, G. S.; Riding, G. H.; Manners, I. *Chem. Mater.* **1990**, *2*, 425.

(20) A preliminary communication including an ORTEP representation of the species $N_3P_3(NMe_2)_4(NH\text{-}B_3N_3Me_5)_2$ appeared in: Welker, M. F.; Manners, I.; Parvez, M.; Allcock, H. R. *J. Chem. Soc., Chem. Commun.* **1989**, 871.

Table I. Characterization Data for Cyclic Borazinylphosphazenes

	^{13}P NMR, ppm		^{11}B NMR, ppm		mass spec		elem anal.		
compound	δ_A	δ_B	δ_A	δ_B	calc	found		calc	found
$N_3P_3Cl_4(NH\text{-}B_3N_3Me_5)_2$ (**3**)	3.93	17.08	36.7	27.6	441	441	C	13.60	13.72
	J = 47.5 Hz						H	3.65	4.12
							N	22.22	21.97
$[NP(NMe_2)(NH\text{-}B_3N_3Me_5)]_3$ (cis,cis,trans, **7a**)	17.61	18.17	36.4	27.4	761	761	C	33.14	32.96
	J = 47.2 Hz						H	8.74	8.33
							N	33.13	33.47
$[NP(NMe_2)(NH\text{-}B_3N_3Me_5)]_3$ (cis,cis,cis, **7b**)	17.28		36.4	27.4	761	761	C	33.14	32.96
							H	8.74	8.33
							N	33.13	33.47
$N_3P_3(NMe_2)_4(NH\text{-}B_3N_3Me_5)_2$ (**10**)	12.25	24.26	36.6	27.5	641	641	C	33.75	33.42
	J = 47.2 Hz						H	8.81	8.95
							N	32.80	32.22
$N_3P_3(OPh)_4(NHB_3N_3Me_5)_2$ (**11**)	12.82	8.01	36.7	27.6	837	837	C	48.81	49.15
	J = 72.9 Hz						H	6.27	5.86
							N	18.42	18.07
$N_3P_3(OPh)_5(OB_3N_3Me_5)$ (**14**)	1.68	9.21	36.0	2.3	766	766			
	J = 74.2 Hz								

to cyclophosphazenes via the formation of either B–P or N–P bonds. In addition, attempts were made to link the rings via short spacer units such as carbon, oxygen, or nitrogen.

The most successful of these routes involved condensation reactions between aminophosphazenes with $-NH_2$ or –NHR side groups and *B*-chloro-*N*-alkylborazines or condensation reactions between chlorophosphazenes and *B*-amino-*N*-alkylborazines. The simplest examples of these reactions are illustrated in Scheme II. Essentially, all these pathways start from hexachlorocyclotriphosphazene (**1**) and involve either replacement of chlorine by the amino unit of an aminoborazine such as *B*-aminopentamethylborazine (**2**) or aminolysis of **1** and subsequent reaction with a chloroborazine such as *B*-chloropentamethylborazine (**5**). The remaining chlorine atoms at the unreacted phosphorus atoms were replaced by subsequent treatment with alkoxides, aryl oxides, or amines, either before or after reaction with the appropriate borazine. This approach yielded a variety of different mixed-substituent (borazinylamino)cyclotriphosphazenes.

The reactions between aminophosphazenes such as the *gem*-diaminotetrachlorocyclotriphosphazene (**4**) and the *B*-chloropentamethylborazine (**5**) took place at room temperature in the presence of a tertiary amine (as hydrohalide acceptor) to give quantitative yields of the corresponding (borazinylamino)cyclophosphazenes such as *gem*-bis(pentamethylborazinyl-*B*-amino)tetrachlorocyclotriphosphazene (**3**). However, the corresponding reactions between **1** and *B*-aminopentamethylborazine (**2**) required longer reaction times and heating to higher temperature (67 °C) to achieve a similar degree of substitution. Furthermore, the reaction between hexachlorocyclotriphosphazene (**1**) and **2** yields only the bis-gem-substituted product (**3**), even after prolonged reaction at 67 °C in THF in the presence of a large excess of **2**.

Geminal disubstitution is known to occur in the reaction of **1** with bulky amines such as aniline or isopropylamine, with the production of higher substitution products upon continued reaction.[15] Unlike the reaction of **1** with aniline, which eventually yields the fully substituted phosphazene, $[NP(NHC_6H_5)_2]_3$, under forcing conditions,[21,22] the replacement of chlorine by aminoborazinyl side groups does not proceed beyond disubstitution, even under forcing conditions. Steric hindrance may contribute to the lack of substitution by aminoborazinyl units beyond the bisgeminal product, since the (pentamethylborazinyl)amino side group is considerably larger than aniline. Nevertheless, these effects are probably not significant, given that most bulky primary and secondary amines react with **1** to yield higher substitution products.[15] In addition, the single-crystal X-ray diffraction structural analysis of the (aminoborazinyl)cyclotriphosphazene (Figure 1, Table II, discussed subsequently) gives no evidence for strong steric interactions. This indicates that the remaining P–Cl bonds must be electronically deactivated following introduction of the first two aminoborazine units. Replacement of the remaining chlorine atoms by stronger nucleophiles such as dimethylamine, sodium phenoxide, and sodium trifluoroethoxide does occur.

A cyclic aminophosphazene bearing three borazinyl side groups in the nongeminal cis,cis,trans configuration can be synthesized via an alternative procedure. Its subsequent rearrangement in solution to the all-nongeminal cis isomer, where all three aminoborazinyl units are on the same side of the phosphazene ring, further indicates that strong steric interactions are not present. Thus, *cis,cis,trans-nongem*-triaminotris(dimethylamino)cyclotriphosphazene, $[NP(NMe_2)(NH_2)]_3$ (**6**), reacts with **5** to yield *cis,cis,trans-nongem*-tris(pentamethylborazinyl-*B*-amino)tris(dimethylamino)cyclotriphosphazene, $[NP(NMe_2)(NHB_3N_2Me_5)]_3$ (**7a**, Chart I). After treatment of a solution of **7a** with triethylamine at 67 °C in THF for 12 h, a mixture of **7a** and the all-cis isomer (**7b**) was formed. The isomerism between the cis,cis,trans and the all-cis configuration has been reported for other mixed substituent aminophosphazene systems,[23] and it reflects the lability of amino side groups in phosphazenes in the presence of ammonium salts.

If the *gem*-diamino species $N_3P_3R_4(NH_2)_2$ (R = NMe_2, **8**; R = OPh, **9**) are employed in place of **4** in the reaction illustrated in Scheme II, the corresponding mixed-substituent *gem*-bis((pentamethylborazinyl-*B*)amino)phosphazenes, $N_3P_3R_4(NH\text{-}B_3N_2Me_5)_2$ (R = NMe_2, **10**; R = OPh, **11**), are produced.

These mixed-substituent (borazinylamino)phosphazenes have been isolated and characterized by ^{11}B and ^{31}P NMR spectroscopy, mass spectrometry and elemental analysis, as summarized in Table I. In addition, the structure of the mixed-substituent *gem*-bis(pentamethylborazinyl-*B*-amino)tetrakis(dimethylamino)cyclotriphosphazene, $N_3P_3(NMe_2)_4(NH\text{-}B_3N_2Me_5)_2$ (**10**), was confirmed by X-ray analysis of a single crystal.

---

(21) Lederle, H.; Ottman, G.; Kober, E. *Inorg. Chem.* **1966**, *5*, 1818.
(22) Bode, H.; Butow, K.; Lienau, G. *Chem. Ber.* **1948**, *81*, 547.
(23) Shaw, R. A.; Keat, R. *J. Chem. Soc.* **1965**, 4067.

Table II. Selected Bond Lengths (Å) and Angles (deg) with Estimated Standard Deviations in Parentheses for the Two Independent Molecules 10a and 10b

	10a	10b		10a	10b
P(1)-N(1)	1.601 (4)	1.568 (6)	P(3)-N(3)	1.614 (6)	1.590 (6)
P(1)-N(3)	1.618 (7)	1.568 (6)	P(3)-N(6)	1.726 (9)	1.613 (7)
P(1)-N(4)	1.644 (6)	1.683 (6)	P(3)-N(7)	1.623 (9)	1.617 (6)
P(1)-N(5)	1.667 (5)	1.664 (6)	B(1)-N(4)	1.38 (1)	1.54 (1)
P(2)-N(1)	1.604 (6)	1.547 (7)	B(1)-N(10)	1.42 (1)	1.47 (2)
P(2)-N(2)	1.595 (8)	1.556 (6)	B(1)-N(12)	1.56 (1)	1.32 (1)
P(2)-N(6)	1.695 (6)	1.587 (9)	B(4)-N(5)	1.48 (1)	1.43 (1)
P(2)-N(7)	1.681 (7)	1.672 (9)	B(4)-N(13)	1.39 (1)	1.45 (2)
P(3)-N(2)	1.632 (6)	1.608 (7)	B(4)-N(15)	1.46 (1)	1.42 (1)
N(4)-P(1)-N(5)	106.3 (3)	105.5 (3)	P(2)-N(2)-P(3)	117.9 (5)	123.8 (3)
N(1)-P(1)-N(3)	116.9 (3)	113.5 (3)	P(1)-N(3)-P(3)	120.6 (3)	123.1 (4)
N(1)-P(2)-N(2)	119.2 (3)	114.1 (3)	P(1)-N(4)-B(1)	139.4 (4)	130.3 (4)
N(2)-P(3)-N(3)	119.3 (3)	114.1 (3)	P(1)-N(5)-B(4)	134.4 (5)	140.6 (5)
P(1)-N(1)-P(2)	120.7 (4)	127.4 (3)			

Chart I

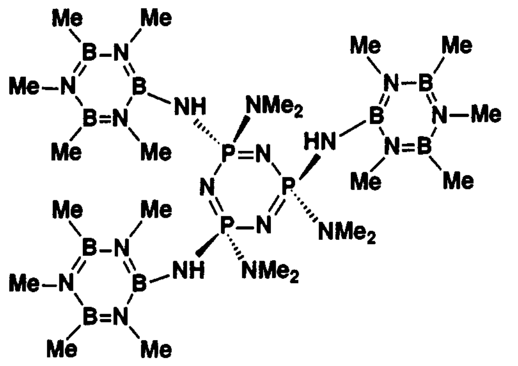

7a

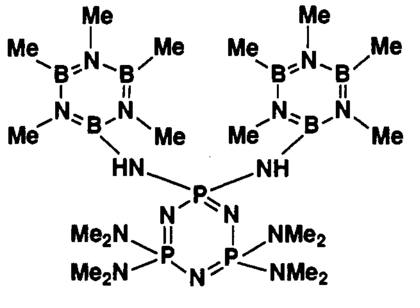

10

Scheme III

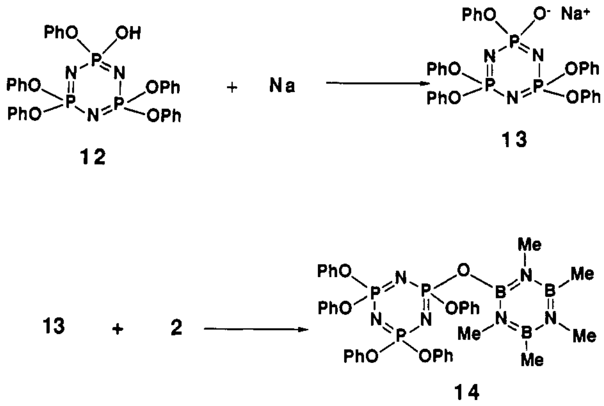

Another possible route to the linkage of borazines to phosphazenes was also examined, as shown in Scheme III. This involved the reaction of sodium oxopentaphenoxycyclotriphosphazene (**13**) with **2**. Analysis of the reaction products by ^{31}P and ^{11}B NMR spectroscopy and mass spectrometry indicated that coupling of the two ring systems occurred. However, the product, pentaphenoxymono(pentamethylborazinyloxo-*B*)cyclotriphosphazene (**14**), was unstable and decomposed rapidly during its attempted isolation.

X-ray Diffraction Studies. A single-crystal X-ray diffraction analysis confirmed the structure of the fully substituted mixed-substituent *gem*-bis(pentamethylborazinyl-*B*-amino)tetrakis(dimethylamino)cyclotriphosphazene, $N_3P_3(NMe_2)_4(NHB_3N_2Me_5)_2$ (**10**). The data are useful for understanding the chemistry of the borazinylphosphazenes, including the structures of the corresponding high polymers.

The analysis indicated the presence of two structurally different molecules, **10a** and **10b**, within the unit cell. The crystal data are as follows: $C_{18}H_{56}N_{15}B_6P_3$, $M = 640.54$, triclinic, space group $P1$, $a = 9.424$ (2) Å, $b = 13.841$ (1) Å, $C = 14.570$ (4) Å, $\alpha = 79.40$ (1)°, $\beta = 83.44$ (2)°, $\gamma = 73.99$ (1)°, $V = 1791.5$ Å^3, $Z = 2$, $D_c = 1.187$ g cm^{-3}, Mo Kα radiation, $\lambda = 0.710\,73$ Å, $\mu = 0.196$ mm^{-1}. $R = 0.066$ for 4412 observed reflections with $I > 3\sigma(I)$ measured on an Enraf-Nonius CAD4 diffractometer at 293 K.

Initial attempts to solve the structure in the centrosymmetric space group, $P\bar{1}$, showed a disordered phosphazene P_3N_3 ring with two P_3N_3 moieties separated by 1.5 Å. This indicated $P1$ as the alternative space group, requiring two independent molecules in the asymmetric unit. The structure was solved by direct methods and was refined successfully in space group $P1$ by full-matrix least-squares calculations allowing anisotropic thermal parameters for the non-hydrogen atoms. The structure of **10a** is shown in Figure 1.[20] The important molecular dimensions of **10a** and **10b** are summarized in Table II.

Several differences between **10a** and **10b** can be seen by examination of Table II. The two independent molecules **10a** and **10b** have significantly different molecular geometries; however, both molecules show several common characteristics. The mean exocyclic B-N bond length (1.46 Å) is similar to the mean endocyclic B-N bond length (1.44 Å), and this indicates a bond intermediate in character between a B-N single and double bond. The comparable lengths of the exocyclic and endocyclic B-N bonds also suggests considerable delocalization throughout these bonds.

The mean exocyclic P-N(borazinylamino) bond length (1.66 Å) is significantly shorter than that of a P(sp^3)-N(sp^3) single bond (1.77 Å),[24] which suggests significant π-character.[25] Although this bond length is notably longer than

---

(24) Hobbs, E.; Corbridge, D. E. C.; Raistrick, B. *Acta Crystallogr.* **1953**, *6*, 621. Cruickshank, D. W. J. *Acta Crystallogr.* **1964**, *17*, 671.

(25) Craig, D. P.; Paddock, N. L. In *Nonbenzenoid Aromatics*.; Academic Press: New York, 1971; Vol. 2.

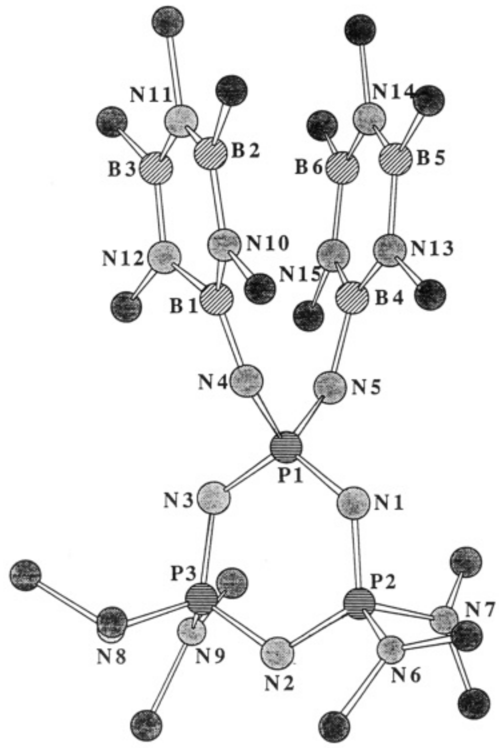

Figure 1. Perspective view of the structure of **10a** showing phosphorus, nitrogen, boron, and carbon. The hydrogen atoms have been omitted for clarity. The molecular structure shown was generated from positional parameters using Chem3D (Cambridge Scientific Computing, Inc., Cambridge, MA).

the average P–N bond length in the phosphazene ring (1.59 Å), it is comparable to the mean exocyclic P–N(dimethylamino) bond length (1.65 Å) of **10**. It is important to note that the exocyclic P–N bonds of secondary amines, such as dimethylamino side groups, are generally longer than the exocyclic P–N bonds of primary amines. Furthermore, dimethylamino side groups are electron releasing into a phosphazene ring and are capable of increasing the length of the other exocyclic bonds that link the phosphazene ring to the other side groups.[15,26,28] In contrast, the short lengths of the exocyclic P–N(borazinylamino) bonds and exocyclic B–N bonds indicate that the borazine ring is able to withdraw electron density from the phosphazene ring. Thus, these observations indicate significant delocalization of the borazinylamino nitrogen lone-pair electrons, with preference into the borazine ring as opposed to the phosphazene ring.

The data also indicate that the molecular structures of **10a** and **10b** are slightly different, presumably a consequence of crystal packing forces. For example, the endocyclic P(1)–N bonds of **10b** (both 1.57 Å) are considerably shorter than those of **10a** (1.60 and 1.62 Å). While the remaining endocyclic P–N bonds of **10b** are also notably shorter, the exocyclic P–N(dimethylamino) bonds of **10b** are only slightly shorter than the corresponding bonds of **10a**.

The borazine rings of each molecule are planar and nearly parallel, with dihedral angles of 15.48 ± 0.65° for **10a** and 13.89 ± 0.74° for **10b**. Both phosphazene rings have slight twist boat conformations. The endocyclic bond angles of **10b** are more distorted than those of **10a** but are similar to those of other unsymmetrically substituted species such as *gem*-$N_3P_3(NH_2)_2(OMe)_4$,[27] *gem*-$N_3P_3Cl_2(NHPr^i)_4$,[28] and $N_3P_3(NMe_2)_6$.[29]

Macromolecular Syntheses. In the following sections different polymers are depicted by bold-faced numbers. However, because of the macromolecular substitution method used for their synthesis, it was possible to vary the ratios of different side groups over a broad range. Thus, polymers with the same side groups are depicted by the same bold-faced number, but different ratios of those side groups are indicated by suffixes **a, b, c....** As stated previously, a primary motive for the synthesis of phosphazenes with borazinylamino side groups was to study the pyrolysis behavior of the polymeric species. Thus, several polymer syntheses were attempted based on the reactions of the cyclic trimers.

Initial efforts to synthesize borazinylaminophosphazene polymers in which every phosphorus atom bore two borazine units were unsuccessful. For example, the reaction the aminoborazine **2** with poly(dichlorophosphazene) (**15**) in various organic solvents and with different reactant stoichiometries and hydrohalide acceptors gave only partially substituted, insoluble polymers. The alternative approach, using the interaction between a reactive poly(aminophosphazene) such as $[NP(NHMe)_2]_n$ and chloroborazine **5** also produced insoluble, partly substituted materials.[30]

It appeared that the problem with this approach stemmed from the high loadings of borazinylamino units along the chain which brought the polymer out of solution before halogen replacement was complete. Thus, subsequent syntheses were designed to reduce the loading of borazine rings on the polymer. This was accomplished by utilizing two different types of side groups in the reactive intermediate. The polymers were prepared with either $-NH_2$ units for reaction with chloroborazines or chloro units for reaction with aminoborazines, as well as unreactive $-NMe_2$ groups to "dilute" the reactive sites along the polymer chains, as illustrated in Scheme IV.

Polymers **16–21**, with 60% or less of the side units as $-NH_2$ groups, were soluble in THF or toluene and were thus appropriate for these studies. However, species containing more than 60% of the side groups as $-NH_2$ units suffered from several problems. Attempts to prepare polymer **17** from polymer **16**, when more than 60% of the side groups were $-NH_2$ units, led to precipitation of the polymer as **17** was being formed. This was probably due to the formation of P–NH–P crosslinks before complete substitution had occurred. Coordination of HCl to the basic nitrogen atoms of the polymer backbone or side groups and hydrogen bonding may also contribute to the formation of insoluble species.

A second problem found for the conversion of **16** and **17** was the displacement of dimethylamino groups by $-NH_2$ groups during the ammonolysis step. For example, if polymer **17a** with 40% dimethylamino side groups, $[NP(NMe_2)_{0.8}(NH_2)_{1.2}]_n$, was exposed to a large excess of ammonia for prolonged periods of time (12 h or longer), the ^{31}P NMR spectrum indicated that only 25% of the dimethylamino side units remained and that the formula was now $[NP(NMe_2)_{0.5}(NH_2)_{1.5}]_n$ (**17c**). This polymer was soluble in THF but became insoluble upon isolation, again probably a consequence of hydrogen bonding in the solid

---

(26) Allen, C. W. In *The Chemistry of Inorganic Homo and Heterocycles*; Haiduc, I., Sowerby, D. B.; Eds.; Academic: London, 1987.

(27) Shaw, R. A.; Shaw, L. S.; Parkes, H. G.; Fincham, J. K.; Hursthouse, M. B. *J. Chem. Soc., Dalton Trans.* **1988**, 1169.

(28) Wagner, A. J.; Polder, W. *Cryst. Struct. Commun.* **1976**, *5*, 253.

(29) Rettig, S. J.; Trotter, J. *Can. J. Chem.* **1973**, *51*, 1295.

(30) The aminophosphazene single-substituent polymer, $[NP(NH_2)_2]_n$, has never been isolated as a well-defined, un-cross-linked macromolecule, presumably because ammonia reacts with poly(dichlorophosphazene) as a difunctional reagent to cross-link the chains.

Scheme IV

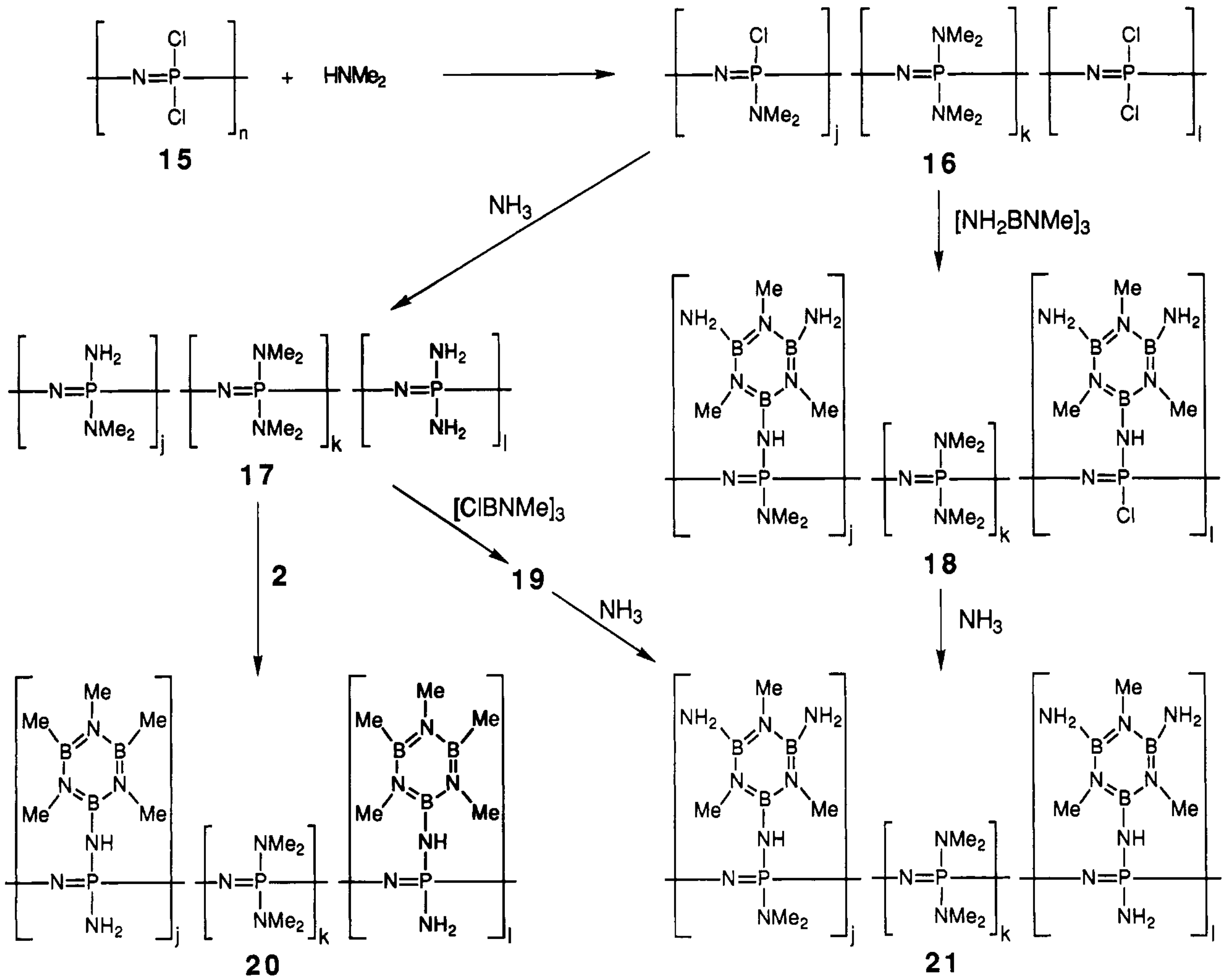

state. The strong basicity of this polymer also prevented complete removal of HCl, as shown by the elemental analyses. Thus, the use of polymer **17** as a reaction intermediate required that at least 40% of the side groups should be dimethylamino units to retard the various modes of cross-linking.

These polymers were hydrolytically sensitive due to the presence of P–NH_2 groups. The borazinyl side units introduced later were also a source of hydrolytic instability. Therefore, all polymers were isolated and purified under anhydrous conditions. Measurements of the molecular weight distributions for these polymers by gel permeation chromatography (GPC) were not feasible due to the hydrolytic sensitivity. However, a fully substituted, hydrolytically stable, dimethylamino single-substituent phosphazene polymer, $[NP(NMe_2)_2]_n$, was synthesized as a model for characterization by GPC methods. This polymer was found to have a M_w above 1×10^6 by comparison with polystyrene standards.

The first fully substituted, mixed-substituent (borazinylamino)phosphazene polymers (**20**) were synthesized by the reaction of **5** with mixed-substituent amino(dimethylamino)phosphazene polymers (**17**). Using polymer **17a** as the intermediate, with 40% of the side groups as dimethylamino units, a maximum incorporation of approximately 35% borazinyl groups was achieved to give the polymer, $[NP(NMe_2)_{0.8}(NHB_3N_3Me_5)_{0.7}(NH_2)_{0.5}]_n$ (**20a**).

The corresponding macromolecules that contained *B*,*B*′,*B*″-triamino(*N*,*N*′,*N*″-trimethylborazinyl) groups (**21**) instead of *B*-amino-*B*′,*B*″-dimethyl-*N*,*N*′,*N*″-trimethylborazinyl groups were also synthesized. The synthesis of mixed substituent (triaminoborazinyl)phosphazene polymers (**21**) is possible through two alternative routes, as illustrated in Scheme IV. The pathway that involved the reaction of *B*,*B*′,*B*″-trichloro-*N*,*N*′,*N*″-trimethylborazine with the mixed-substituent aminodimethylamino polymer **17** requires an additional step compared with the reaction of *B*,*B*′,*B*″-triaminoborazine with the partially substituted dimethylamino polymer **16**, but the route via **17** yielded polymers with up to 10% higher incorporation of borazinyl groups.

The linkage of aminoborazinyl groups via intermediate polymer **17** may be slightly easier than via **18** because steric hindrance effects may be less severe if the reaction site is one unit further removed from the backbone. Second, as noted for the small-molecule syntheses, the reaction of a cyclic chlorophosphazene with aminoborazines deactivates the phosphazene toward further substitution. Thus, more forcing conditions are required, and the reaction does not yield products with as high a loading of aminoborazinyl side groups as the reactions of chloroborazines with aminophosphazenes.

The structures of polymers of types **16**–**21** were examined by a combination of several methods, including ^{31}P and ^{1}H NMR spectroscopy, elemental analysis, thermogravimetric analysis (TGA), and X-ray photoelectron spectroscopy (XPS). The side group ratios were estimated by integration of the ^{31}P NMR resonances. The assignment of phosphorus nuclei to the corresponding peaks in the high-field ^{31}P NMR is given in Table III. High-field ^{31}P NMR spectra for a typical reaction sequence, the

Table III. Assignment of Phosphorus Nuclei Corresponding to Resonances in the High-Field ^{31}P NMR Spectra of Polymers 16–21

phosphorus nuclei (side-group environment)[a]	peak assignment, ppm
$P(NH_2)_2$	18.4
$P(NHB_3N_3R_2Me_3)(NH_2)$	16.4
$P(NHB_3N_3R_2Me_3)_2$	14.9
$P(NMe_2)(NH_2)$	7.8
$P(NHB_3N_3R_2Me_3)(NMe_2)$	1.5
$P(NHB_3N_3R_2Me_3)Cl$	−1.3
$P(NMe_2)_2$[b]	6.5 (**16a**)
	−7.0 (**20c**)
$P(NMe_2)Cl$	−9.3
PCl_2[b]	−18.0 (**15**)
	−26.0 (**16a**)

[a] R = CH_3 or NH_2. [b] The resonance for these phosphorus nuclei depends upon the cosubstituents present. Figure 2 shows representative spectra for the polymers referenced parenthetically, with the exception of the chlorophosphazene starting polymer, $(NPCl_2)_n$ (15), which is identified by ^{31}P NMR as a singlet at −18.0 ppm.

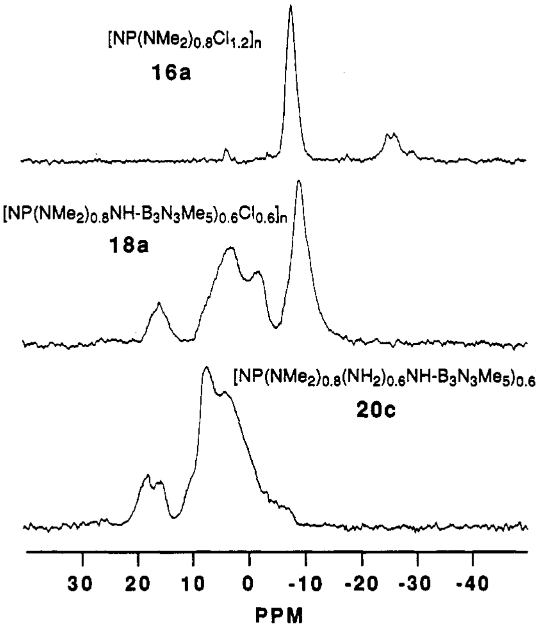

Figure 2. High-field ^{31}P NMR spectra for (top to bottom) $[NP(NMe_2)_{0.8}Cl_{1.2}]_n$ (**16a**), $[NP(NMe_2)_{0.8}(NHB_3N_3Me_5)_{0.6}Cl_{0.6}]_n$ (**18a**), and $[NP(NMe_2)_{0.8}(NH_2)_{0.6}(NHB_3N_3Me_5)_{0.6}]_n$ (**20c**).

synthesis of $[NP(NMe_2)_{0.8}(NH\text{-}B_3N_3Me_5)_{0.6}(NH_2)_{0.6}]_n$ (**20c**) via the polyphosphazene intermediates $[NP(NMe_2)_{0.8}Cl_{1.2}]_n$ (**16a**) and $[NP(NMe_2)_{0.8}(NHB_3N_3Me_5)_{0.6}Cl_{0.6}]_n$ (**18a**), are shown in Figure 2. ^1H NMR spectroscopy could not be used to accurately determine the abundance of the specific side groups in these polymers because of the overlap and breadth of the resonances. Moreover, reproducible elemental analyses of these polymers could not be obtained because of the incomplete combustion. However, the elemental analyses indicated the presence of boron, carbon, nitrogen, and hydrogen. These results are shown in the Experimental Section.

Pyrolysis Studies. The pyrolysis of polymers 17, 20, and 21 resulted in ultrastructure materials in the form of residual brown, black, or gray cross-linked solids and sometimes orange chemical vapor deposition products. The thermal characteristics of these polymers were examined by thermogravimetric analysis (TGA), gas chromatography (GC), and gas chromatography/mass spectroscopy (GC/MS), Fourier transform infrared spectroscopy (IR), X-ray photoelectron spectroscopy (XPS), and powder X-ray diffraction (XRD). These analytical techniques were used to study the volatile products, the factors influencing their elimination, and the composition and character of the ultrastructure materials generated by pyrolysis.

Table IV. Summary of Thermogravimetric Analysis Results

polym mol formula	onset temp, °C	approx wt loss, %	final ceram yield, %
$[NP(NMe_2)_{0.8}(NH_2)_{1.2}]_n$ (**17a**)	gradual < 700	50	
	920	45	<5
$[NP(NMe_2)_{1.2}(NH_2)_{0.8}]_n$ (**17b**)	310	45	
	920	35	7
$[NP(NMe_2)_{1.4}(NHB_3N_3Me_5)_{0.6}]_n$ (**20b**)	450	85	<5
$[NP(NMe_2)_{0.8}(NH_2)_{0.6}(NHB_3N_3Me_5)_{0.6}]_n$ (**20a**)	220	50	
	850	10	20
$[NP(NMe_2)_{0.8}(NH_2)_{0.5}(NHB_3N_3\{NH_2\}_2Me_3)_{0.7}]_n$ (**21a**)	gradual < 500	15	
	600	25	55

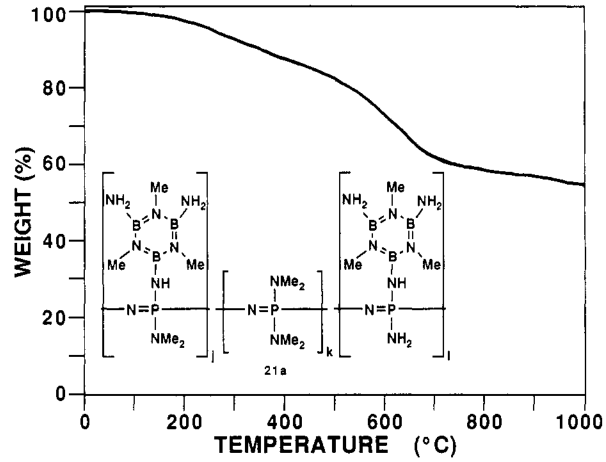

Figure 3. Thermogravimetric analysis weight loss for the pyrolysis of $[NP(NMe_2)_{0.8}(NH_2)_{0.5}(NHB_3N_3\{NH_2\}_2Me_3)_{0.7}]_n$ (**21a**) under argon.

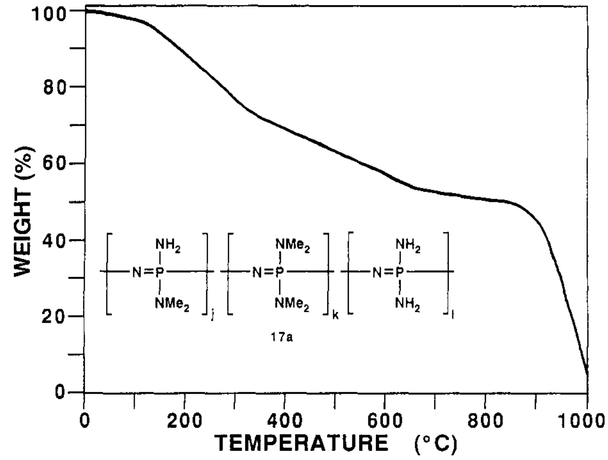

Figure 4. Thermogravimetric analysis weight loss for the pyrolysis of $[NP(NMe_2)_{0.8}(NH_2)_{1.2}]_n$ (**17a**) under argon.

The TGA analyses were carried out by heating a sample (5–12 mg) of each polymer to 1000 °C at a heating rate of 2–10 °C/min under nitrogen. Several polymers with different ratios of side groups were compared in order to assess the contribution of each side group to the resultant thermal behavior of these mixed-substituent polyphosphazenes. The results of these analyses are summa-

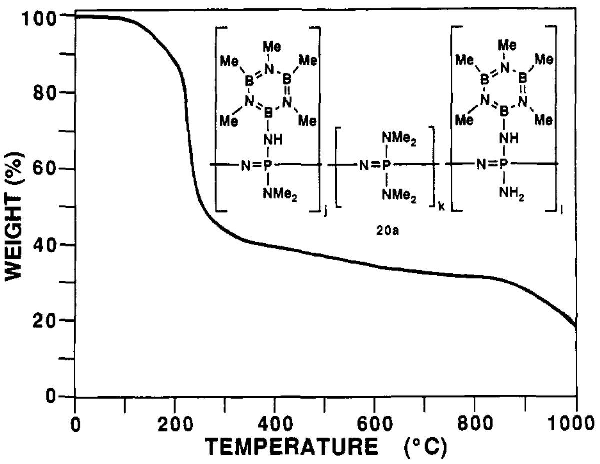

Figure 5. Thermogravimetric analysis weight loss for the pyrolysis of $[NP(NMe_2)_{0.8}(NH_2)_{0.5}(NHB_3N_3Me_5)_{0.7}]_n$ (**20a**) under argon.

rized in Table IV. The thermograms of polymers **21a**, **17a**, and **20a** are shown in Figures 3–5, respectively. The thermogram of polymer **21a** revealed the highest percentage of residue after pyrolysis (55%). Attempts to increase the ceramic yield from this polymer by isothermal heating at intermediate temperatures improved the yield only marginally to 57%. The bulk pyrolysis of polymer **21a**, with the molecular formula $[NP(NMe_2)_{0.8}(NHB_3N_3\{NH_2\}_2Me_3)_{0.7}(NH_2)_{0.5}]_n$, and polymer **17a**, with the molecular formula $[NP(NMe_2)_{0.8}(NH_2)_{1.2}]_n$, were carried out under ammonia, nitrogen, or (more frequently) argon atmosphere in a tube furnace to yield samples of residual cross-linked materials, volatile gases, and chemical vapor deposition products for further analysis.

The data in Table IV clearly indicate the importance of unreacted $-NH_2$ groups, both linked directly to the polymer backbone and attached to the borazinyl rings, for generating a high ceramic yield. The thermolysis residue from the polymer with *B*-aminopentamethylborazinyl side groups (**20a**) was only 20% at 1000 °C, while that of a similar polymer that contained *B,B′,B″*-triamino-*N,N′,N″*-trimethylborazinyl side groups (**21a**) was 55%. Furthermore, a polymer with no $-NH_2$ side groups linked directly to the skeletal phosphorus, $[NP(NMe_2)_{1.4}(NHB_3N_3Me_5)_{0.6}]_n$ (**20b**, $l = 0$) sustained a more dramatic (85%) weight loss at a moderate onset temperaure (450 °C) than did polymers **20a** or **21a** (60% and 15% weight loss below 500 °C, respectively) and virtually complete volatilization of the pyrolysis products by 1000 °C (less than 5% yield vs 20% and 55%).

The dramatic weight loss of polymers **20a** and **20b** at moderate temperatures reflects the relative size and weight of the *B*-aminopentamethylborazinyl side group. Volatilization of the borazinyl side group represents a major weight loss relative to the formula weight of the parent polymer (**20a**, 98.8 amu/188.6 amu, 52%; **20b**, 98.8 amu/205.5 amu, 48%). Analysis of the volatile products by gas chromatography and gas chromatograph/mass spectroscopy showed *B*-aminopentamethylborazine, *B*-(methylamino)pentamethylborazine, and dimethylamine as the major volatile byproducts below 500 °C. These studies indicate that thermolytic elimination of a pentamethylborazine is preferred to cross-link formation via a borazinyl linkage. This is in sharp contrast to polymer **21a** with *B,B′,B″*-triaminoborazinyl side groups, as discussed later in this paper.

The importance of incorporating *B,B,B*-triaminoborazinyl groups in order to obtain a high ceramic yield is also evident upon examination of the data in Table IV and Figures 3–5. Figure 4 shows the thermogram of the borazine-free polymer **17a** with the molecular formula $[NP(NMe_2)_{0.8}(NH_2)_{1.2}]_n$. A gradual weight loss took place up to 700 °C, with approximately 50% weight retention at that temperature. The weight loss in this temperature range is characteristic of side-group loss and formation of P–NH–P and P–NMe–P cross-links. Analysis of the volatile byproducts by gas chromatography and gas chromatograph/mass spectroscopy showed ammonia, monomethylamine, and dimethylamine as the major byproducts. Rapid weight loss occurred above 800 °C, and this indicates a facile breakdown of the polymer backbone and the loss of small-molecule volatile species.[19] During the bulk pyrolysis of this polymer in a tube furnace, the weight loss which occurred between 800 and 1000 °C corresponded to orange chemical vapor deposition (CVD) products. These CVD byproducts deposited on quartz slides in the 300–500 °C region of the tube. Infrared analysis (820–940, 1000–1150 cm^{-1}) and X-ray photoelectron spectroscopy (P(1s), 133 eV; N(1s), 398 eV) indicate that these CVD products are primarily phosphorus nitride and are similar to phosphorus nitride CVD products of other pyrolyzed aminophosphazenes.[19]

Figure 3 depicts the thermogram of borazine-containing polymer **21a** with the molecular formula $[NP(NMe_2)_{0.8}(NHB_3N_3\{NH_2\}_2Me_3)_{0.7}(NH_2)_{0.5}]_n$. This polymer undergoes a gradual decrease in weight (15%) below 550 °C and a more obvious decrease in weight (25%) between 550 and 700 °C due to the loss of side-group residues. Analysis of the volatile byproducts by gas chromatography and gas chromatograph/mass spectroscopy showed ammonia, monomethylamine, and dimethylamine as the major volatile byproducts below 700 °C; only very small amounts of borazine residues were observed. Furthermore, **21a** is significantly more stable at temperatures above 700 °C, with only an additional 5% weight loss occurring between 700 and 1000 °C. The incorporation of *B,B′,B″*-triaminoborazinyl groups in polymer **21a** causes an 11-fold increase in the ceramic yield over the comparison polymer **17a**. The *B,B′,B″*-triaminoborazinyl side groups inhibit the volatilization of the polymer backbone via cross-linking reactions between the borazine ring, amino substituents, and the polymer backbone. As noted for polymer **17a** and other polyaminophosphazenes,[19] weight loss in the region between 700 and 1000 °C is associated with volatilization of the phosphorus and nitrogen of the polymer backbone and the corresponding chemical vapor deposition of phosphorus nitride; no CVD products were deposited during the pyrolysis of polymer **21a**.

The side groups at boron on the borazinyl ring also influence the thermal stability of these polymers. A polymer that contained no unreacted $-NH_2$ groups on the borazinyl rings, $[NP(NMe_2)_{0.8}(NHB_3N_3Me_5)_{0.7}(NH_2)_{0.5}]_n$ (**20a**, Figure 5), had a lower thermal stability than did **21a** (Figure 3). Polymer **20a** undergoes a rapid weight loss (50%) during heating to 250 °C and continued gradual weight loss (25%) up to 1000 °C with only 20% ceramic yield. This is indicative of a facile loss of side group residues below 250 °C, followed by degradation of the macromolecular backbone and volatilization of the low molecular weight fragments between 250 and 1000 °C. When heated to 1000 °C, the polymer that contained *B,B′,B″*-triamino-*N,N′,N″*-trimethylborazinyl side groups with reactive B–NH_2 units (**21a**, Figure 3) resulted in a 35% improvement in the final ceramic yield compared with the corresponding polymer with pentamethylborazinyl-*N*-amino side groups (**20a**, Figure 5). It is also important that polymer **20a**, which lacks unreacted B–NH_2 groups, still

Table V. Chemical Composition (Atom %) of the Solid Pyrolysis Residues from X-ray Photoelectron Spectroscopic Analysis

init polym	pyrolysis temp, °C	pyrolysis gas	P	B	N	C	O	Si	Al	F	approx mol formula
17a	1000	Ar	5.34	0.00	16.56	74.92	2.33	0.63	0.00	0.22	PN_3C_{14}
21a	1000	Ar	1.52	29.22	25.55	16.36	24.80	1.20	1.35	0.00	$PN_{17}B_{19}C_{10}$
21a	1000	NH_3	1.78	33.41	31.69	16.28	15.12	1.36	0.36	0.00	$PN_{18}B_{19}C_9$
21a	1300	Ar	0.00	36.27	36.51	14.40	10.45	0.83	0.00	1.54	B_3N_3C

showed a 4-fold increase in the ceramic yield compared with the corresponding polymer that contained no borazinyl side groups, $[NP\text{-}(NMe_2)_{0.8}(NH_2)_{1.2}]_n$ (**17a**, Figure 4).

Perhaps the most significant result from the pyrolysis studies is that the highest ceramic yields occurred when the polymeric precursor contained unreacted $-NH_2$ groups on *both* the polymer backbone and the borazinyl side units. Precursor polymers that lack both unreacted $B-NH_2$ units and unreacted $P-NH_2$ units (for example, **20a** and **20b**) gave significantly lower ceramic yields. This indicates that P–NH–B cross-link formation at low-to-moderate temperatures is important. These cross-links limit the loss of borazinyl side groups below 500 °C and minimize the loss of small-molecule volatile species formed by the breakdown of the polymer backbone at higher temperatures. Other cross-linking units, such as B–NH–B, P–NH–P, P–NMe–P, P–NMe–B, and P–CH–N may also be formed, but their contribution to the ceramic yield of these polymers is probably less significant.

It is also noteworthy that, even when $B-NH_2$ units are absent, the borazine side groups still exert a retarding effect on the loss of weight as the temperature is raised. Previous studies have postulated that bulky side groups can increase the thermal stability of polyphosphazenes, since intramolecular steric hindrance may inhibit cyclization–depolymerization reactions.[19,31–33] However, the latent thermal reactivity of the polymer side groups must also contribute significantly to the enhanced thermal stability of these polymers. For example, polymers such as $[NP(CH_3)(C_6H_5)]_n$ and $[NP(OC_6H_5)_2]_n$ are known to depolymerize to cyclic oligomers below 300 °C. Although the poly(methylphenylphosphazene) volatilizes completely below 500 °C, the polyphenoxyphosphazene retains 7% of its original weight at 1000 °C. In contrast, $[NP(NHC_6H_5)_2]_n$ retains 33% of its weight at 1000 °C, nearly a 5-fold improvement over the phenoxy derivative. The improved weight retention of the polymer, as the side group is changed from phenyl to phenoxy to anilino, is attributed to the increased ability of the respective side group to undergo condensation processes at moderate temperatures, generating the cross-links required to prevent extensive structural breakdown at elevated temperatures. Likewise, the enhanced thermal properties of the (*B*,*B*′,*B*″-triaminoborazinyl)polyphosphazenes described in this paper are due in part to the low volatility of borazine–phosphazene thermolysis fragments as well as their steric inhibition of depolymerization but are primarily a consequence of the latent thermal reactivity of the *B*,*B*′,*B*″-triaminoborazinyl groups at moderate and elevated temperatures, generating a stabilized, highly cross-linked, three-dimensional matrix.

Samples (1–2 g) of polymers **21a**, with the molecular formula $[NP(NMe_2)_{0.8}(NHB_3N_3\{NH_2\}_2Me_3)_{0.7}(NH_2)_{0.5}]_n$, and **17a**, with the molecular formula $[NP(NMe_2)_{0.8}(NH_2)_{1.2}]_n$, were pyrolyzed in a tube furnace to yield samples of residual cross-linked materials, volatile gases, and chemical vapor deposition (CVD) materials for analysis. The polymer samples were heated at 5–10 °C/min to 1000 °C, under an atmosphere of either argon or nitrogen. There were no significant differences between the analyses of the residual cross-linked materials, volatile gases, or chemical vapor deposition materials produced under a flow of either argon or nitrogen. Polymer **21a** was heated similarly to 1300 °C and then isothermally heated at this temperature for 10 h. In addition, polymer **21a** was pyrolyzed to 1000 °C under an anhydrous ammonia atmosphere. The residues, CVD products, and volatiles from these pyrolysis experiments were analyzed by elemenetal analysis and X-ray photoelectron spectroscopy (XPS), gas chromatography (GC), gas chromatography/mass spectrometry (GC/MS), infrared Fourier transform spectrometry (IR), and powder X-ray diffraction (XRD). The elemental analyses yielded only limited information due to incomplete combustion, but significant amounts of nitrogen, boron, and carbon were detected.

The XPS analyses were integrated to give the atomic concentrations. A summary of the atomic concentrations for phosphorus, boron, nitrogen, carbon, oxygen, silicon, and fluorine and an approximate molecular formula based on phosphorus, boron, nitrogen, and carbon are given in Table V. Although the argon and ammonia atmosphere sources for these pyrolyses were very pure (Ar = 99.9995%) and all pyrolysis precursors and products were handled under an inert atmosphere and stored in a drybox, oxygen was present on the surface of the pyrolyzate in significant concentrations (2–25%). The oxygen probably arises from the unavoidable exposure of the samples to the atmosphere for 5–10 s during transfer to the antechamber of the XPS instrument. Indeed, deliberate exposure of samples to the atmosphere for days generated surface oxygen concentrations of 50%. Surface contamination is also possible via contact with the quartz pyrolysis tube, ceramic pyrolysis boat, or the Teflon-coated instruments used in handling the pyrolysis residues (aluminum, silicon, and fluorine were also found in small amounts, with the aluminum found only in samples pyrolyzed in the ceramic container). The presence of oxygen in these residues is probably not indicative of the bulk composition. XPS is strictly a surface analysis, and the results suggest that an oxide coating is formed rapidly. This is common for many non-oxide ceramics such as boron nitride.[34,35] The presence of silicon, aluminum, fluorine, and oxygen in the surface layers suggests strongly that the ceramic products are still highly reactive, even after being heated to 1300 °C and cooled to ambient temperature under an inert atmosphere.

The XPS analyses of the residue from the pyrolysis to 1000 °C of polymer **17a** (Figure 5) indicated the presence of phosphorus nitride (P(1s), 133 eV; N(1s), 398 eV). Polymer **21a** (Figure 6) yielded phosphorus nitride and boron nitride (B(1s), 190 eV; N(1s), 398 eV).[33] XPS analysis of the residue from polymer **21a** pyrolyzed to 1300

---

(31) Fewell, L. L.; Basi, R. J.; Parker, J. A. *J. Appl. Polym. Sci.* **1983**, *28*, 2659.

(32) MacCullum, J. R.; Tanner, J. *Macromol. Sci., Part A* **1970**, *4*, 481.

(33) Goldfarb, L.; Hann, N. D.; Dieck, R. L.; Messersmith, D. C. *J. Polym. Sci., Polym. Chem. Ed.* **1978**, *16*, 1505.

(34) Wagner, C. D.; Riggs, W. M., Davis, L. E., Moulder, J. F., Muilenberg, G. E., Eds. *Handbook of X-ray Photoelectron Spectroscopy*; Perkin-Elmer Corp.: Eden Prairie, MN, 1979.

(35) Rye, R. R.; Tallant, D. R.; Paine, R. T.; Lindquist, D. A.; Borek, T. T. *Chem. Mater.* **1991**, *3*, 286.

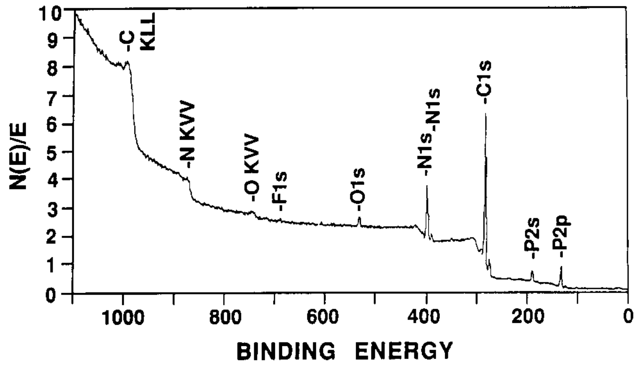

Figure 6. X-ray photoelectron spectrum of the pyrolysis residue from $[NP(NMe_2)_{0.8}(NH_2)_{1.2}]_n$ (**17a**, T = 1000 °C, argon).

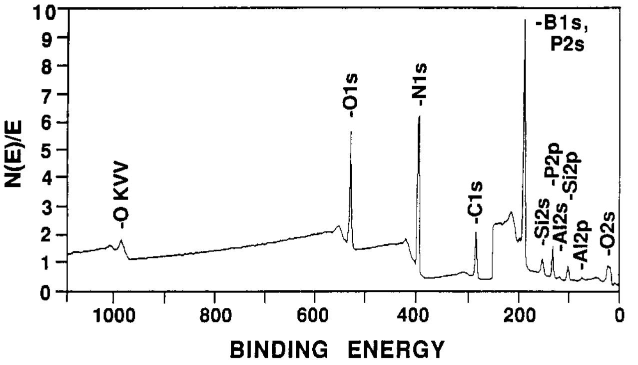

Figure 7. X-ray photoelectron spectrum of the pyrolysis residue from $[NP(NMe_2)_{0.8}(NH_2)_{0.5}(NHB_3N_3\{NH_2\}_2Me_3)_{0.7}]_n$ (**21a**, T = 1000 °C, argon).

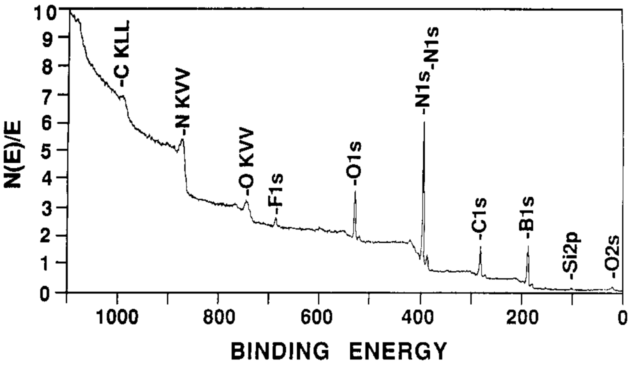

Figure 8. X-ray photoelectron spectrum of the pyrolysis residue from $[NP(NMe_2)_{0.8}(NH_2)_{0.5}(NHB_3N_3\{NH_2\}_2Me_3)_{0.7}]_n$ (**21a**, T = 1300 °C, argon).

°C (Figure 7), though still carbon and oxygen rich, showed a significant loss of carbon and no remaining phosphorus, and this indicated a nearly complete conversion to boron nitride.

The black ceramic solids from the pyrolysis to 1000 °C of polymer **17a** were amorphous by powder X-ray diffraction (XRD). Although the solid residues from polymer **21a** pyrolyzed to 1000 °C (black solids with small, isolated, light brown areas) were also largely amorphous by XRD, broad diffraction lines were attributable to the presence of BN. The width (>2°) and weak intensity of these lines suggest that only a relatively small fraction of the solid is crystalline or partially crystalline BN. Continued pyrolysis of polymer **21a** to 1300 °C resulted in light brown/black to gray solids. The XRD analysis of these solids showed improved resolution of the relatively broad diffraction lines. The *d* values for these solids, 3.4 (002) and 2.1 (100, 101), compare well with the literature data for hexagonal (sometimes referred to as turbostratic) boron nitride.[13,36,37]

Experimental Section

Reagents. All synthesis experiments were carried out with the reactants under an atmosphere of dry argon or nitrogen. The pyrolyses were conducted under argon (Matheson) of 99.9995% purity. Tetrahydrofuran was freshly distilled under nitrogen from sodium benzophenone ketyl. Chlorobenzene was freshly distilled under nitrogen from P_2O_5. Triethylamine, toluene, hexane, and acetonitrile were freshly distilled from CaH_2 under nitrogen. Sodium (Aldrich), sodium hydride (Aldrich), dimethylamino (Matheson), ammonia (Matheson), and boron trichloride (Aldrich) were used as received. Hexachlorocyclotriphosphazene (1) was obtained from a trimer–tetramer mixture (Ethyl Corp.) and was purified by recrystallization from hexane, followed by two fractional sublimations. Methylammonium chloride (Aldrich) was purified by sublimation.

Analytical Instrumentation. ^1H, ^{31}P, and ^{11}B NMR spectra were obtained with the use of Varian EM-360, CFT-20, Bruker WP-200 MHz FT, or JEOL FX 90Q NMR spectrometers. Positive chemical shifts for ^{31}P and ^{11}B NMR are downfield from the external references (0.00 ppm) of 85% H_3PO_4 and $BF_3{\cdot}Et_2O$, respectively. Electron impact mass spectra were obtained by means of an AEI MS 950 instrument. The molecular weights of the polymers were estimated by gel permeation chromatography (GPC) with the use of a Hewlett-Packard HP 1090 liquid chromatograph equipped with a refractive index detector. Polymer Laboratories PLgel (10^6, 10^6, 10^3 Å) columns were calibrated with narrow molecular weight polystyrene standards. Elemental analyses were obtained by Galbraith Laboratories, Knoxville, TN. Volatile byproducts were analyzed by using a Varian 3700 gas chromatograph (GC) and a Finnigan gas chromatograph/mass spectrometer (GC/MS). A Perkin-Elmer 1710 infrared Fourier transform spectrometer was used to obtain infrared (IR) spectra. X-ray photoelectron spectra (XPS) were obtained at the Perkin-Elmer Corp., Physical Electronics Division Laboratories, Edison, NJ, using a Perkin-Elmer 5500 Multitechnique system. The samples were mounted in an inert-atmosphere glovegox using double-sided tape and then quickly transferred into the system. The spectra were obtained using monochromatic aluminum X-ray radiation (Al Kα = 1486.6 eV) operated at 500 W. Atomic composition data were determined by using the instruments computer and programmed sensitivity factors. The powder X-ray diffraction (XRD) spectra were recorded on a Rigaku diffractometer.

Thermogravimetric Analyses of the Polymer Systems. Thermogravimetric analyses were recorded on a Perkin-Elmer TGA-7 unit equipped with a PE 7500 computer. The polymer samples (5–10 mg) were analyzed under a constant flow (25 cm^3/min) of nitrogen in an iridium pan (the (aminoborazinyl)phosphazene breakdown products reacted with platinum and gold pans) at variable heating rates (0–10 °C/min). The thermograms presented in this paper (Figures 3–5) were acquired using a heating rate of 5 °C/min from room temperaure to 1000 °C. The instrument was calibrated using the magnetic standards alumel (163 °C), nickel (354 °C), and perkalloy (596 °C).

Preparative Scale Pyrolysis of the Polymers in a Tube Furnace. The samples were placed on a quartz slide or in a ceramic boat, which was then inserted into a quartz flow tube and heated in a Lindberg 55035A tube furnace. The entire pyrolysis was carried out under a constant flow (25–30 cm^3/min) of anhydrous gas (either argon, nitrogen, or ammonia). The samples (1–2 g) were heated from 25 to 1000 or 1300 °C at a rate of 5–10 °C/min. The temperatures within the quartz tube and downstream of the heated zone were calibrated by means of a Cole Parmer Digi-Sense unit with type K thermocouple. Fractions of the volatile byproducts were collected in a trap cooled to −196 °C and analyzed by gas chromatography and gas chromatography/mass spectrometry.

Preparation of Known Compounds. Compounds **2**,[34] **4**,[35] **5**,[36] **6**,[37] **8**,[37] **9**,[38] **12**,[39] **15**,[40] $(ClBNMe)_3$,[41] and $(NH_2BNMe)_3$[34] were

---

[36] Thomas, J.; Weston, N. E.; O'Connor, T. E. *J. Am. Chem. Soc.* **1963**, *84*, 4619.

[37] *Inorganic Powder Diffraction File*; Berry, L. G., Ed.; Joint Committee on Powder Diffraction Standards: Swarthmore, 1990, and references therein.

[38] Toeniskoetter, R. H.; Hall, F. R. *Inorg. Chem.* **1963**, *2*, 29.

prepared and characterized by procedures described in the literature.

Preparation of *gem*-Bis(pentamethylborazinyl-*B*-amino)tetrachlorocyclotriphosphazene (3). Small-molecule model compounds **3**, **7a**, **7b**, **10**, and **11** were prepared by one of two different methods, by either the reaction of chlorocyclotriphosphazenes with aminoborazines or aminocyclotriphosphazenes with chloroborazines. A typical procedure developed for the reaction of cyclic chlorophosphazenes with aminoborazines is given below.

To a 250-mL three-necked flask equipped with an addition funnel and reflux condenser were added **1** (5.00 g, 14.3 mmol), **2** (7.50 g, 45.3 mmol), THF (100 mL), and $N(CH_2CH_3)_3$ (10 mL). The reaction mixture was heated to reflux for 24 h and was then allowed to cool to room temperature. The solvent was removed under reduced pressure with heating. The residue was redissolved in toluene, and the alkylammonium chloride salts were removed by gravity filtration through a fine glass frit. The excess borazine was removed by sublimation (65 °C, 0.1 Torr). Recrystallization from CH_2Cl_2/hexane gave **3** as colorless crystals. Yield 4.6 g (73%). Calculated for $C_{10}H_{32}N_{11}P_3B_6$: C, 13.60; H, 3.65; N, 22.22. Found: C, 13.72; H, 4.12; N, 21.97.

Preparation of *gem*-Bis(pentamethylborazinyl-*B*-amino)tetraphenoxycyclotriphosphazene (11) and Related Compounds. Small-molecule model compounds **3**, **7a**, **7b**, **10**, and **11** were also prepared by the reaction of aminocyclotriphosphazenes with chloroborazines. The preparation and characterization of **10** has been reported previously.[20] A typical procedure developed for the reaction of cyclic aminophosphazenes with chloroborazines is given below.

A 250-mL three-necked flask equipped with an addition funnel and reflux condenser was charged with **9** (5.00 g, 9.27 mmol), **5** (5.10 g, 27.6 mmol), THF (100 mL), and triethylamine (10 mL). The reaction mixture was heated to reflux for 6 h and then allowed to cool to room temperature. The solvent was removed under reduced pressure with heating. The residue was redissolved in toluene, and the triethylammonium chloride was removed by gravity filtration through a fine glass frit. The excess borazine was removed by sublimation (65 °C, 0.1 Torr). Recrystallization from CH_2Cl_2/hexane gave **11** as colorless crystals. Yield 6.3 g (81%). Calculated for $C_{34}H_{52}O_4N_{11}P_3B_6$: C, 48.81; H, 6.27; N, 18.42. Found: C, 49.15; H, 5.86; N, 18.07.

Attempted Reaction between 13 and 2. Compound **13** was prepared from **12** (1.00 g, 1.62 mmol) in THF (50 mL) in a 100-mL three-necked flask equipped with an addition funnel by use of methods reported in the literature.[41] A solution of **2** (0.60 g, 3.24 mmol) in THF (25 mL) was added via the addition funnel. Mass spectrometric analysis (calculated and found, 766), ^{11}B NMR ($\nu_A = 2.3$ ppm, $\nu_B = 36.0$ ppm), and ^{31}P NMR ($\nu_A = 1.68$ ppm, $\nu_B = 9.21$, $J_{AB} = 74.2$ Hz) provided evidence that species **15** was formed in the reaction mixture. However, it proved to be too labile to be isolated.

Preparation of Partially Substituted Poly((dimethylamino)chlorophosphazene) (16a) and Related Macromolecules. Polymer **15** (10.00 g, 86.2 mmol) was dissolved in THF (1000 mL) in a 2000-mL three-necked flask equipped with an addition funnel cooled by a dry ice/acetone bath and a reflux condenser. The polymer solution was cooled to 0 °C, and a solution of dimethylamine (3.11 g, 69.0 mmol) in THF (200 mL) and triethylamine (25 mL) was added dropwise via the addition funnel. After complete addition of the dimethylamine solution, the reaction mixture was allowed to warm to room temperature, was subsequently heated to reflux for 6 h, and then was allowed to cool to room temperature. The solution was concentrated to approximately 400 mL, and the precipitated salts were removed by suction filtration through a course glass frit. The solution was concentrated to approximately 150 mL, and the polymer was precipitated into hexane. Purification of **16a** was carried out by repeatedly redissolving the recovered polymer in toluene, filtration through a course glass frit, followed by precipitation into hexane (two times). The purified polymer was dried under vacuum (2 × 10^{-6} mmHg) for 24 h to give 7.9 g (75% yield) of a white elastomer. A ^{31}P NMR spectrum was consistent with the structure $[NP(NMe_2)_{0.8}Cl_{1.2}]_n$ for **16a** (Figure 2).

Preparation of Mixed-Substituent Poly(amino(dimethylamino)phosphazene) (17a) and Related Polymers. To a 2000-mL three-necked flask, equipped with an airless addition funnel and a dry ice/acetone coldfinger condenser were added ammonia (100 g, 6.30 mol), THF (300 mL), and triethylamine (50 mL). Polymer **16a** (4.00 g, 32.6 mmol) was dissolved in THF (500 mL) and was transferred to the airless addition funnel for subsequent addition to the ammonia solution. The addition took place over 1 h. Stirring was continued for an additional hour, and the condenser was then removed. Solvent and excess ammonia were volatilized under reduced pressure with heating. The solution was concentrated to approximately 400 mL and the precipitated salts were separated by suction filtration through a course glass frit. The solution was concentrated to approximately 100 mL and precipitated into hexane. The residue was redissolved in toluene (100 mL), and residual alkylammonium chloride salts were removed by suction filtration through a course glass frit. Purification of **17a** was carried out by repeatedly redissolving the recovered polymer in toluene, filtering through a course glass frit, and then precipitating into hexane (two times). The purified polymer was dried under vacuum (2 × 10^{-6} mmHg) for 24 h to give 1.8 g (56% yield) of a white elastomer. The ^{31}P NMR spectrum was consistent with the formula, $[NP(NMe_2)_{0.8}(NH_2)_{1.2}]_n$, for **17a**.

Preparation of Mixed-Substituent Poly(amino(dimethylamino)(borazinylamino)polyphosphazene), $[NP(NMe_2)_{0.8}(NHB_3N_3\{NH_2\}_2Me_3)_{0.7}(NH_2)_{0.5}]_n$ (21a) and Related Compounds. Polymers **20** and **21** can be prepared by either of two similar procedures: by the reaction of mixed-substituent amino(dimethylamino)polyphosphazenes **17** with chloroborazines or by the reaction of partially substituted chloro(dimethylamino)polyphosphazenes **16** with aminoborazines. Both routes involve a subsequent reaction with ammonia to replace the remaining chlorine atoms at boron or phosphorus. A typical procedure for the reaction of the mixed substituent amino(dimethylamino)polyphosphazene **17a** with *B,B′,B″*-trichloroborazine is as follows.

B,B′,B″-Trichloro-*N,N′,N″*-trimethylborazine (20.0 g, 88.5 mmol) was dissolved in a mixture of THF (500 mL) and triethylamine (50 mL) using a 1000-mL three-necked flask equipped with an addition funnel and reflux condenser. After this solution was heated to reflux, **17a** (1.00 g, 10.1 mmol) in THF (150 mL) was added dropwise via the addition funnel. After complete addition of the polymer solution, the reaction solution was heated to reflux for an additional 24 h and the mixture was then allowed to cool to room temperature. The solution was concentrated to approximately 100 mL, and the precipitated salts were removed by suction filtration through a course glass frit. The polymeric intermediate, $[NP(NMe_2)_{0.8}(NHB_3N_3Cl_2Me_3)_{0.7}(NH_2)_{0.5}]_n$ (**19a**), was recovered by three precipitations from THF into acetonitrile. It was then redissolved in THF.

A 1000-mL three-necked flask equipped with an airless addition funnel and a dry ice/acetone coldfinger condenser was charged with ammonia (50 g, 3.15 mmol), THF (200 mL), and triethylamine (25 mL). Polymer **19a** in THF (300 mL) was transferred to the addition funnel for subsequent addition to the ammonia solution. The addition took place over 1 h. Stirring was continued for an additional hour, and the condenser was then removed. Solvent and excess ammonia were removed under reduced pressure with heating. The solution was concentrated to approximately 200 mL, and the precipitated salts were separated by suction filtration through a course glass frit. The solution was concentrated to approximately 50 mL and was then precipitated into hexane. The residue was redissolved in toluene (50 mL), and residual alkylammonium chloride salts were removed by suction filtration through a course glass frit. Polymer **21a** was recovered

---

(39) Feistel, G. R.; Moeller, T. *J. Inorg. Nucl. Chem.* **1967**, *29*, 2731.

(40) Ryschkewitsch, G. E.; Harris, J. J.; Sisler, H. H. *J. Am. Chem. Soc.* **1958**, *80*, 4515.

(41) Allcock, H. R.; Kolich, C. H.; Kossa, W. C. *Inorg. Chem.* **1977**, *16*, 3362.

(42) McBee, E. T.; Okuhara, K.; Morton, C. J. *Inorg. Chem.* **1966**, *5*, 450.

(43) Fitzsimmons, B. W.; Hewlett, C.; Hills, K.; Shaw, R. A. *J. Chem. Soc. A* **1967**, 679.

(44) Allcock, H. R.; Kugel, R. L.; Valan, K. J. *Inorg. Chem.* **1966**, *5*, 1709.

(45) Haworth, D. T. *Inorg. Synth.* **1972**, *13*, 43.

Chem. Mater. **1992**, *4*, 307-312 307

by repeated precipitations from a filtered toluene solution into acetonitrile (two times) and hexanes (two times). The polymer was dried under vacuum (2×10^{-6} mmHg) for 48 h. Integration of the peaks from a ^{31}P NMR spectrum indicated that the molecular formula was $[NP(NMe_2)_{0.8}(NHB_3N_3\{NH_2\}_2Me_3)_{0.7}(NH_2)_{0.5}]_n$. Yield 0.93 g (45%). Elemental analysis calculated for $[NP\text{-}(NMe_2)_{0.8}(NHB_3N_3\{NH_2\}_2Me_3)_{0.7}(NH_2)_5]_n$: C, 21.69; H, 7.67; N, 37.6; B, 11.08. Found: C, 20.21; H, 6.96; N, 24.33; B, 24.33, Cl, <2.5.

Preparation of Mixed-Substituent Poly(dimethylamino)borazinylamino)polyphosphazene) $[NP(NMe_2)_{1.4}(NHB_3N_3Me_5)_{0.6}]_n$ (20b) and Related Compounds. Compound **2** (15.0 g, 90.6 mmol) was dissolved in a mixture of THF (500 mL) and triethylamine (50 mL) using a 1000-mL three-necked flask equipped with an addition funnel and reflux condenser. After heating this solution to reflux, **16a** (1.00 g, 10.1 mmol) in THF (150 mL) was added dropwise via the addition funnel. After complete addition of the polymer solution, the reaction solution was heated to reflux for an additional 24 h, and the mixture was then allowed to cool to room temperature. The integrated peak areas from the ^{31}P NMR spectrum for the resultant polymer (**18a**, Figure 2) were consistent with the molecular formula $[NP(NMe_2)_{0.8}(NHB_3N_3Me_5)_{0.6}Cl_{0.6}]_n$. The reaction flask was equipped with a dry ice/acetone condenser. A large excess of dimethylamine (50.0 g, 1.11 mol) was condensed into the reaction flask, and the mixture was stirred with the condenser in place for 12 h. The solution was concentrated to approximately 75 mL, and the precipitated salts were removed by suction filtration through a course glass frit. Polymer **20b** was recovered by repeated precipitations from a filtered toluene solution into acetonitrile (two times) and hexanes (two times). The polymer was dried under vacuum (2×10^{-6} mmHg) for 48 h. The integrated peak areas from the ^{31}P NMR spectrum were consistent with the formula $[NP\text{-}(NMe_2)_{1.4}(NHB_3N_3Me_5)_{0.6}]_n$. Yield 1.3 g (54%).

Acknowledgment. We thank the U.S. Air Force Office of Scientific Research for the support of this work. We also thank Lawrence Salvati of Perkin-Elmer Corp. for the XPS data.

Registry No. **1**, 940-71-6; **2**, 89417-01-6; **3**, 138957-41-2; **5**, 13058-05-4; **7a**, 138957-44-5; **7b**, 139066-30-1; **9**, 5032-83-7; **10**, 138957-45-6; **11**, 138957-42-3; **13**, 138957-43-4; **14**, 138957-46-7; **15**, 26085-02-9.

Rietveld Analysis of $Na_xWO_{3+x/2}\cdot yH_2O$, Which Has the Hexagonal Tungsten Bronze Structure

Kenneth P. Reis,† E. Prince,‡ and M. Stanley Whittingham*,†

Department of Chemistry and Materials Research Center, State University of New York at Binghamton, Binghamton, New York 13902-6000, and Materials Science and Engineering Laboratory, National Institute for Standards and Technology, Gaithersburg, Maryland 20899

Received July 16, 1991. Revised Manuscript Received December 3, 1991

Powder neutron diffraction and Rietveld analysis were used to investigate the crystal structures of hydrated and deuterated samples of $Na_xWO_{3+x/2}\cdot yH_2O$ ($x \sim 0.17, y \sim 0.23$). The compound, which crystallizes with the symmetry of space group *P6/mmm*, is related to the hexagonal tungsten bronze structure but differs from it due to the presence of sodium and oxygen along the hexagonal tunnel. Some of the oxygens appear in the structure as water molecules. The oxygen is disordered along the *z* axis in the hexagonal cavity with sodium in the hexagonal window.

Introduction

The tungsten bronzes have the general formula M_xWO_3, where M is normally a monovalent cation. The tungsten bronzes crystallize in four different structural types: perovskite, tetragonal I, hexagonal tungsten bronze, and intergrowth tungsten bronzes. The structure of the bronze obtained depends upon the size and amount of the alkali metal. The hexagonal tungsten bronze (HTB), where $0.19 \le x \le 0.33$, normally forms with the largest cations (M = K, Rb, Cs, Tl, NH_4). The tungsten bronzes have free electrons and are metallic conductors.

During the past 2 decades, there have been reports of completely oxidized compounds that appear to have the hexagonal tungsten bronze structure. These tungstates tend to have the general formula $M_xWO_{3+x/2}$. The compounds sharing this formula include $K_2W_8O_{25}$ and $K_2W_6O_{19}$.[1,2] The potassium formulas can be written as $K_{0.25}WO_{3.125}$ and $K_{0.33}WO_{3.165}$ to show their relationship to the hexagonal bronzes more easily. The compound, $BiTaW_2O_{10}$, is another oxidized version of the tungstates.[3] These compounds are of interest because the alkali-metal cation, and the additional oxygen must lie along the one-dimensional hexagonal tunnel. Attempts at solving the structures by X-ray analysis of single crystals have not succeeded in locating all the atoms.[3,4] For the potassium phases, oxygen could not be located in the hexagonal tunnel. In $BiTaW_2O_{10}$, bismuth and oxygen were forced into positions that gave an unrealistic Bi–O bond distance.[3]

The potassium tungstates are known to undergo the redox reaction

$$K_xWO_3 \leftrightarrow K_xWO_{3+x/2}$$

This reaction indicates that the oxygen atoms diffuse in and out of the hexagonal tunnel. (The 123-superconductor undergoes a similar type redox reaction.) To date, it is not yet understood how the oxygen diffuses in and out of the hexagonal tunnel. The problem is that the oxygen must

---

† State University of New York at Binghamton.

‡ National Institute for Standards and Technology.

* To whom all correspondence should be sent.

(1) Deschanvres, A.; Desgardin, G.; Raveau, B.; Thomazeau, J. C. *Bull. Soc. Chim. Fr.* 1967, 4537.

(2) Hussain, A.; Kihlborg, L.; Klug, A. *J. Solid State Chem.* **1978**, *38*, 189.

(3) Deschanvres, A.; Leparmentier, L.; Raveau, B. *Bull. Soc. Chim. Fr.* 1971, 3459.

(4) Klug, A. *Mater. Res. Bull.* 1977, *12*, 837.

0897-4756/92/2804-0307$03.00/0